Analysis of the Timetable Impact on Energy Consumption of a Subway Line

Ryan Berriel, Philippe Delarue, Clément Mayet, Alain Bouscayrol, Charles Brocart

Analysis of the Timetable Impact on Energy Consumption of a Subway Line

Ryan O. Berriel, Philippe Delarue, Clément Mayet, Alain Bouscayrol and Charles Brocart

***Abstract*—This paper analyzes the timetable impact on the energy consumption of a subway line. In most timetable studies, simplified models are used and can lead to misestimation of the braking energy and thus the energy transfer between braking vehicles and accelerating vehicles. In this paper, specific attention is paid to the models of the vehicles, the traction power substation, and the rail supply network to enable an accurate estimation of the energy consumption. The energetic macroscopic representation formalism is used to organize the models of the subsystems so they have the right interactions. The developed model is validated by experimental tests on a real subway line. The error on the global energy consumption is lower than 2.2%. The model is then employed to examine the influence of the vehicle time interval on energy consumption. A 10-second adjustment in this time interval can result in a substantial 22% decrease in energy consumption for the analyzed real subway line.**

***Index Terms*—Regenerative braking, timetable, subway simulation, energetic macroscopic representation.**

I. Introduction

SUBWAY systems are widely used in metropolitan areas. They play a key role in mobility in even more urbanized societies [1]. The advantages of subway systems can be described as punctuality, low greenhouse gas emissions, and low consumption per passenger-kilometer [2]. This mode of transportation is constantly expanding.

In order to mitigate the increasing power demand and energy consumption, its operation is widely studied [3], [4]. In terms of propulsion, subway vehicles are traditionally electrified. Thus, regenerative braking capability is a natural consequence. Traction power substations (TPSs) are used to feed the rail supply system. It is generally composed of a transformer in series with a diode rectifier. Therefore, the vehicles are commonly supplied with direct current (DC). This topology implies a network with a non-reversible characteristic.

Many solutions are studied in order to reduce the energy consumption of subway lines [5]. Therefore, an important amount of braking energy can be recovered [6]. The first method is to integrate reversible TPS to reinject this energy in the AC grid [7]. The second way is to integrate energy storage subsystems [8], in the vehicles (on-board) [9], [10] or in the infrastructure level (wayside) [6], [11]. Another possibility is to act on the timetable, i.e. the time interval between the vehicles [12]. In this solution, the regenerative braking energy is reused by subways accelerating [13]. Moreover, eco-driving is also considered [14]. Acting on the timetable is a relevant solution since there is no need to change the infrastructure or add new technologies. However, the synchronization of the subways is a complex task due to the numerous parameters to consider.

Timetable optimization is thus an important research area for the reduction of energy consumption of subway lines at a lower cost when compared to the integration of energy-saving technologies [15]. In a subway carousel system, vehicles are injected at the line terminus respecting a certain interval. The schedule operation of the subway is divided into time slots where the interval between vehicles is adjusted to meet a certain demand. In this approach, fixed intervals are expected on each station, resulting in a periodic timetable [16].

To meet the passenger demand on peak-hours, the interval between vehicles injection is considerably reduced. For instance, in the Line 1 of the city of Lille (France), during peak-hours the interval is reduced to 66 seconds. In contrast, 360 seconds is imposed during certain slots of a regular day when passenger demand is lower. This operation is different from some rail transit systems [17] where the magnitude of the interval can reach tens of minutes and the passenger flow has more impact on the accumulation of passenger on platforms [18], [19]. For the carousel subway system, the demanded interval between vehicles is predefined by the operator and is selected considering statistical data and the passenger comfort. Consequently, by changing the interval between vehicles the synchronization of braking and acceleration phases is modified.

The rail supply line is the element that connects the different vehicles on braking and acceleration phases. It is often simplified or neglected. The methodology in most of the work considers the line as a single ideal conductor [20] and regenerative braking energy is shared between accelerating and braking vehicles on the line. In [21], a distance range is fixed to determine the utilization of generative braking energy by accelerating vehicles and energy storage devices. In [22], regenerative braking energy can only be absorbed by successive trains which belong to the same substation section. Another approach consists in the calculation of the overlapping time of acceleration and braking vehicles [23], where transmission losses are typically neglected.

Many algorithms have been proposed to define optimal timetables [21], [24], [25]. All these studies are based on simplified traction system models that enable the optimization process [26]. A backward approach is generally used where all velocity profiles are considered possible despite some mechanical and electrical limitations [27]. However, these constraints may prevent reaching the desired final position, leading to inaccuracies in the actual energy consumption estimation.

In [28], the maximization of regenerative braking energy is

proposed by the use of dynamic programming techniques. In the work, an improved velocity profile is obtained and imposed on the system. However the dynamics of the filter capacitor is neglected and the impact of the TPS and rail supply system is not considered.

In [29], a framework is proposed for real-time cooperation of a multi-train system with the objective of minimizing the net energy consumption. The vehicle model is simplified and transmission losses are also ignored on the system model.

In [30], a energy-saving strategy based on static power conditioner with the energy storage system is presented. In this paper, the mathematical model of the vehicle is simplified and the power demanded is based on punctual measurements and imposed independent of the environmental conditions.

In contrast, this paper proposes a different approach to model and analyze timetable optimization problems. A casual approach is used where the supply line is represented as a electrical circuit problem. The circuit configuration is updated on each time step respecting the position between vehicles and TPSs. In this methodology, the energy flow calculation between all the subsystems that compose the network is a natural consequence.

In order to guarantee the right energy consumption evaluation of the vehicle traction system, a forward approach including the capacitor model is considered. The forward approach consists in controlling the system to dynamically adjust velocity and accurately reach the destination, and thus obtain the real energy consumption [31].

Furthermore, while simplified models may not take into account the dynamics of the input filter capacitor, it is an important factor to consider. The voltage of the capacitor is a crucial variable in determining the proper functioning of the system. The capacitor voltage on vehicle model guarantee a reference voltage for the rail supply circuit solution. This consideration opens the possibility to determine the voltage level on every point of the supply line. This is particular important to properly implement mechanical braking activation rules [32] and to determine charging and discharging strategy of energy storage devices [33]. This approach guarantees that excess of energy is properly dissipated, thus, a dynamical model of the capacitor enables the right estimation of the energy consumption.

Accordingly, the objective of this paper is to analyze the timetable effect on the energy consumption of a subway line. A perspective of the evolution of energy consumption in function of the interval is given, which support the development of optimization algorithms. The subway line 1 of the city of Lille (France) is considered as example. The model of subway vehicles has been developed in [34] and a model of the TPS is now added. The model of the supply rail network interconnects different TPS and vehicles and transmission losses are now included. The complete model is validated by experimental results on the real line. The use of a more complex model is justified as it allows better evaluation of the energy flow within the vehicle and between the elements that comprise a subway line.

The subway line of the city of Lille has been previously studied in a forward approach with dynamical models [35]

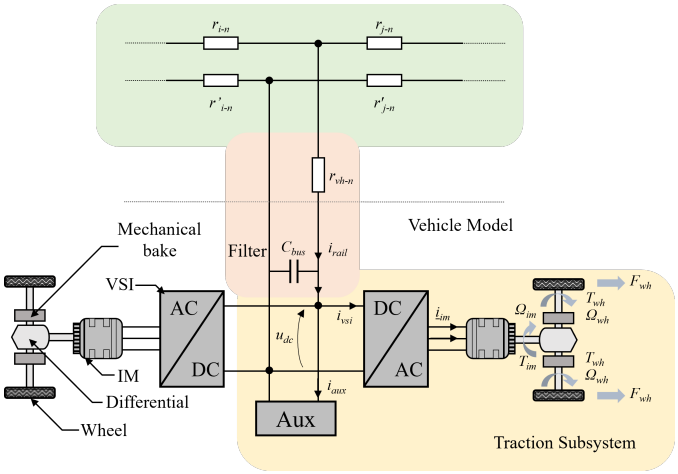

Fig. 1. Structure of the subway traction system.

[31]. This study with Siemens subways has compared two solutions in order to double the capacity of passengers (i.e. double the number of cars in a vehicle or double the number of vehicles on the track). A new subway is now integrated by Alstom with vehicles composed of 4 cars instead of 2 cars [36]. The simulation model of the new vehicle has been validated and analyzed to be integrated with a line simulation [34]. All these studies have been organized using the EMR (Energetic Macroscopic Representation) formalism [37]. EMR is a graphical description of complex energy conversion systems and their control. As EMR is based on the interaction principle, the connection of different parts of a subway line will ensure the right interaction between them. The exchanged power is highlighted between subsystems and energy flow can be better analyzed.

Section II deals with the models of the subsystems that compose a subway line. Section III presents the experimental validation of the vehicle model. In Section IV, energy consumption is studied for different timetables.

II. Subway Line Model

A subway line can be divided into three main subsystems: the vehicle, the TPS, and the supply rail (Fig. 1). The studied automatic subway is developed by Alstom for the city of Lille (France). In traction mode, the electrical energy from the TPS is converted into mechanical energy. In braking mode, part of the mechanical energy is recovered to the supply rail network.

The traction model has been already presented in [36]. Now, the TPS model is added as well as the rail model to have a complete subway line.

A. Vehicle Model

The subway vehicle is composed of 3 traction cars and 1 non-traction car. All 4 cars are equipped with mechanical braking. Each traction car is composed of 2 electrical drives and 4 driven wheels (Fig. 1). More details are given in [36].

A dynamical model of the vehicle has been developed in [36] and experimentally validated. A simplified model using a static model of the electric drive has been derived. For the LC

filter, only the capacitor is kept as its voltage is a key variable for blocking the TPS and for activating the mechanical system, as clearly explained in [35].

For the simulation of a subway carousel, several vehicles are simulated simultaneously. Consequently, if dynamical model is used the total simulation time becomes impracticable. Indeed, as the dynamical model requires a small integration step time, a quasi-static model [35] is preferred for studying multiple vehicles. An equivalent wheel is also considered where curves and slipping phenomena are neglected. A common mechanical brake is used and the modeling the non-traction car avoided.

In the study presented in [34], different models for the vehicle have been examined. The implementation of a simplified model has shown to significantly reduce computation time by 51%, while only resulting in a minimal 2% deviation in energy consumption. Consequently, the high accuracy of this model is confidently assured. A comprehensive comparison of different EMRs can be found in [34], with the chosen EMR for this research illustrated in Fig. 2. Furthermore, the filter capacitor is now considered as the connection point with the supply line in the present study.

The filter capacitor is depicted by an accumulation element (crossed orange rectangle) with the voltage u_{dc} as output. This voltage is obtained from the rail and load current, i_{rail} and i_{load}:

$$i_{rail} - i_{load} = C'_{bus} \frac{du_{dc}}{dt}. \tag{1}$$

With C'_{bus} the capacitance. The load current is the combination of the car currents i_{car}, assuming the 3 cars have the same current (adaptation element, oranges square with >):

$$i_{load} = 3\, i_{car}. \tag{2}$$

Each car current is the sum of the traction and auxiliary current, i_{trac} and i_{aux} (coupling element, orange double square):

$$i_{car} = i_{trac} + i_{aux}, \quad \text{with} \quad i_{aux} = P_{aux} \frac{1}{u_{dc}}, \tag{3}$$

where P_{aux} is the auxiliary power demand, a source element (green oval). As there are 2 electric drives in a car, the traction current is a combination (adaptation element) of the drive currents i_{vsi}:

$$i_{trac} = 2\, i_{vsi}. \tag{4}$$

A static model of an electric drive is considered [35] and is represented by a multi-domain conversion element (orange circle). The torque T_{im} follows instantaneously its reference T_{im-ref}. The drive current i_{vsi} is obtained from the torque, rotational speed Ω_{im}, DC link voltage and electrical drive efficiency η_{dr}

$$\begin{cases} i_{vsi} = \frac{T_{im}\Omega_{im}}{\eta_{dr}^{\delta} u_{dc}} \\ T_{im} = T_{im-ref} \end{cases} \quad \text{with} \quad \delta = \begin{cases} 1, & \text{when } T_{im}\Omega_{im} > 0 \\ -1, & \text{when } T_{im}\Omega_{im} \leq 0. \end{cases} \tag{5}$$

For the differential gearbox (conversion element), the ratio K_d and efficiency η_d determine the expression for the differential gear torque T_{gb} and rotational speed Ω_{wh}

$$\begin{cases} T_{gb} = K_d \eta_d^{\delta} T_{im} \\ \Omega_{im} = K_d \Omega_{wh} \end{cases} \quad \text{with} \quad \delta = \begin{cases} 1, & \text{when } T_{im}\Omega_{im} > 0 \\ -1, & \text{when } T_{im}\Omega_{im} \leq 0. \end{cases} \tag{6}$$

The differential (conversion element) decomposed the torque into 2 equivalent torques T_{wh}

$$T_{wh} = \frac{T_{gb}}{2}. \tag{7}$$

For the wheel (conversion element), the radius R_{wh} determines the traction force F_{wh} and velocity v_{vh}

$$\begin{cases} F_{wh} = \frac{1}{R_{wh}} T_{wh} \\ \Omega_{wh} = \frac{1}{R_{wh}} v_{vh}. \end{cases} \tag{8}$$

Adaptation elements are used to describe the wheel, bogie, and car contribution to the traction force. The combination of the force on wheels determines the bogie resultant force F_{bg} as

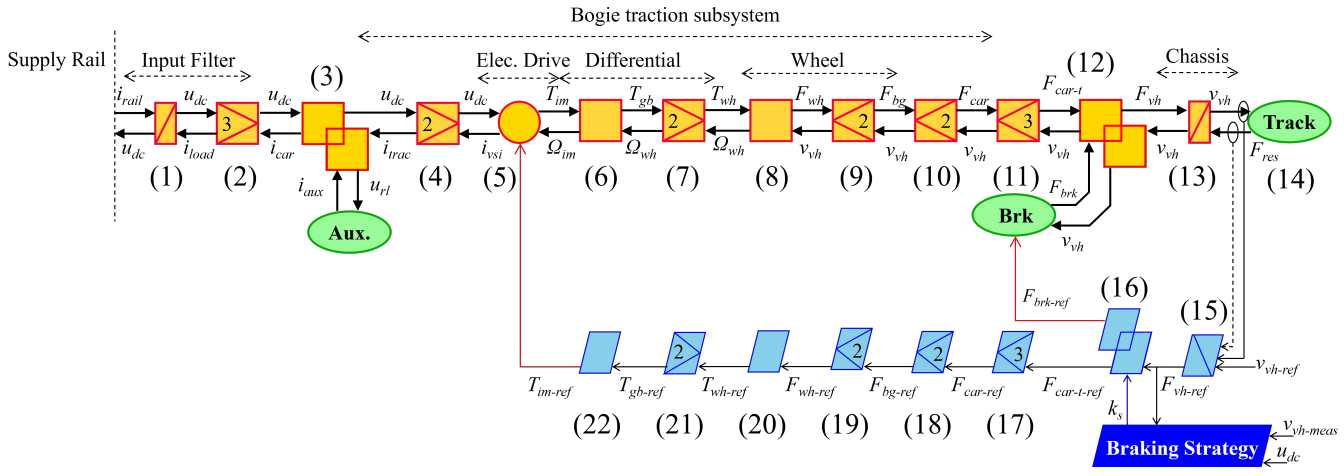

Fig. 2. EMR and inversion-based control of the subway vehicle.

$$F_{bg} = 2\,F_{wh}. \tag{9}$$

The traction car force F_{car} is determined by the number of bogies (two per car)

$$F_{car} = 2\,F_{bg}. \tag{10}$$

Finally, the force contribution of all three traction cars F_{car-t} is stated as

$$F_{car-t} = 3\,F_{car}. \tag{11}$$

The mechanical brake is represented by a source element that imposes the brake force F_{brk}. A coupling element is used to represent the combination of traction and braking force. The vehicle resultant force F_{vh} is described by

$$F_{vh} = F_{car-t} + F_{brk}. \tag{12}$$

The chassis is depicted by an accumulation element with the velocity depending on the vehicle and resistive F_{res}

$$\frac{dv_{vh}}{dt} M_{vh} = F_{vh} - F_{res}, \tag{13}$$

where M_{vh} is the dynamical mass of the subway.

The resistive force F_{res}, imposed by the track, is defined as a function of the velocity, number of cars N_{cars}, static mass M^s_{vh}, gravitational acceleration g, slope θ, drag coefficient D, rolling resistance B and static force F_0

$$F_{res} = N_{cars}F_0 + Bv_{vh} + Dsign[v_{vh} - v_w](v_{vh} - v_w)^2 + \theta g M^s_{vh}. \tag{14}$$

In terms of control, the objective is to impose the velocity v_{vh-ref}. Therefore, a control structure is deduced from the EMR according to the inversion rules [37].

The chassis inversion requests a closed-loop control (light blue crossed parallelogram) to define the force reference F_{vh-ref}

$$F_{vh-ref} = C_v(t)(v_{vh-ref} - v_{vh-meas}) + F_{res-meas}, \tag{15}$$

where $C_v(t)$ is the controller (proportional-integral or other kind).

In braking mode, a part of the force demand can be applied using mechanical brakes instead of regenerative braking. For that, a variable k_s is defined to determine the share of the reference force that is applied using mechanical brakes and electrical brakes $F_{car-t-ref}$

In braking mode, this force is distributed in mechanical and recovery braking, $F_{bfk-ref}$ and $F_{car-ref}$, using this distribution variable k_s:

$$\begin{cases} F_{brk-ref} = k_s F_{vh-ref} \\ F_{car-t-ref} = (1 - k_s) F_{vh-ref}. \end{cases} \tag{16}$$

For safety reasons, pure mechanical braking is ensured when the vehicle is stopped with a smooth transition below 5 km/h [36]. Moreover, the distribution is also dependent on the DC line: pure mechanical braking is provided for 950V with a smooth transition between 850V and 950V (Fig. 3). In traction mode k_s is imposed to 0. During the operation k_s is updated at each simulation step time according to the voltage of the train DC bus. Therefore, the sharing between regenerative and dissipation braking is ensured and updated at each time according to the line receptivity.

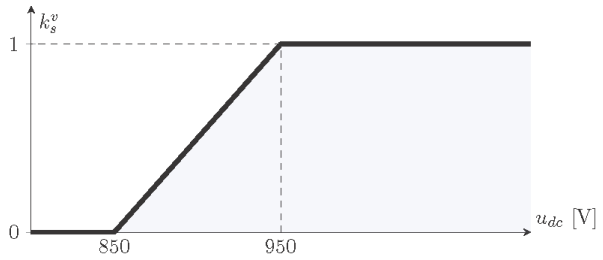

Fig. 3. Coefficient for mechanical braking activation vs. DC bus voltage.

During the braking phases, the implemented strategy ensures that the required efforts can be applied by the machine set. The variable k_s is also influenced by the electrical machine operating point in order to prevent it from exceeding its limits.

Adaptation and conversion elements are directly inverted from their equation to deliver step-by-step the torque T_{im-ref}

$$F_{car-ref} = \frac{1}{3} F_{car-t-ref}; \tag{17}$$

$$F_{bg-ref} = \frac{1}{2} F_{car-ref}; \tag{18}$$

$$F_{wh-ref} = \frac{1}{2} F_{bg-ref}; \tag{19}$$

$$T_{wh-ref} = R_{wh} F_{wh-ref}. \tag{20}$$

$$T_{gb-ref} = 2 T_{wh-ref} \tag{21}$$

$$T_{im-ref} = \frac{1}{K_d} T_{gb-ref}. \tag{22}$$

B. Traction Power Substation Model

The TPS is responsible for powering the rail supply system. The considered structure is composed of a power transformer in series with a diode rectifier. Thus, it is a nonlinear element. Simplified models are often proposed for numerical advantages [38], [39]. In this work, it is considered a static model. In previous study, different TPS models has been analyzed and it shows that the selected model has a deviation of only 0.8% on energy consumption when compared to a more complex model [32]. In the study conducted in [40], simplified models are examined in the context of evaluating the trade-off between accuracy and computational costs. Simplified models are proposed as an effective approach for analyzing energy consumption while mitigating computational demands.

The TPS can assume two possible states: conduction mode (ON) and blocked mode (OFF).

In conduction mode, the observed voltage at the TPS point of connection is equal or lower than the rectified nominal

voltage. In this case, the model is considered an ideal voltage source. Its value is constant and equal to the rectified nominal voltage.

The blocked mode refers to a situation where the voltage at the TPS point of connection is higher than its nominal rectified voltage. This can occur due to an high number of vehicles braking simultaneously and insufficient electrical power consumption on the network. In this scenario, the rail supply voltage reference is provided by the vehicle filter capacitor. The capacitor, as a storage device, has a voltage that fluctuates as it charges and discharges, which in turn affects the voltage along the supply rail. In blocked mode, the TPS is considered to be a zero current source. This means that the TPS does not provide or consume any current, but instead acts as a passive element in the electrical circuit. The voltage at the TPS point remains observed and is crucial to determine the operation mode.

Hence, the switching state depends on the current and voltage at the connection point. The blocked mode is activated when the current has a zero or negative value. The conduction mode is activated when the TPS voltage is greater than the nominal voltage [32]. The considered EMR of the TPS is depicted in Fig. 4.

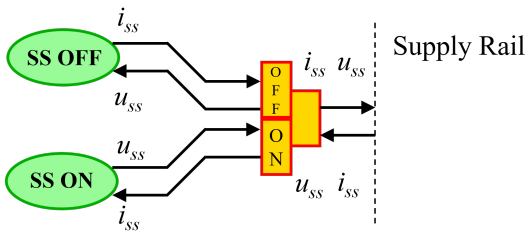

Fig. 4. The EMR of a TPS.

C. Railway Track Model

The rail supply network works as a transmission line that operates as a power interface between the TPSs and the vehicles in both directions. It is a long conductor with an equivalent linear resistance Λ_{rail} $[\Omega/m]$. An example of a circuit structure is depicted in Fig. 5.

In the resulting network, the resistance between two generic subsystems A and B can be calculated as:

$$r_{AB} = \Lambda_{rail}|x_A - x_B|, \tag{23}$$

where x_A and x_B represent the position of the subsystems A and B respectively. As a vehicle moves along the line, its equivalent resistance between other subsystems is variable. Differently, the position is fixed for each TPS.

Additional factors, such as linear inductance and parasitic capacitance, can be taken into account for the rail supply model. However, the study in [32] demonstrates that a static model with only linear resistance results in 99.2% accuracy in energy consumption, making it sufficient for this work. Additionally, in [41], it is demonstrated that the pure resistive

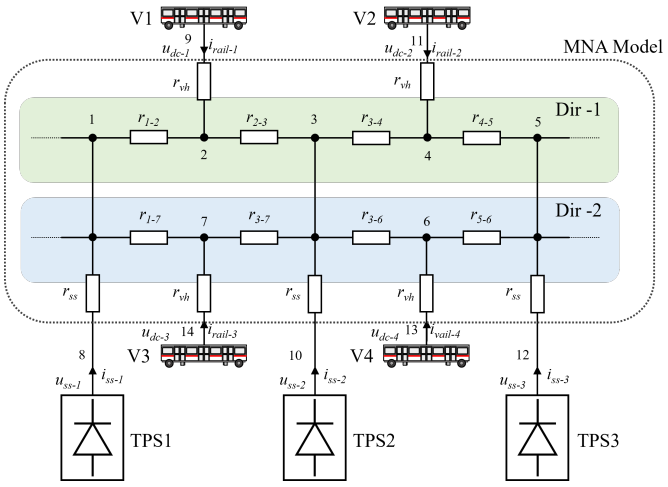

Fig. 5. Circuit representation of a subway line.

model is widely accepted as an effective method for studying DC railway supply lines.

For the subway line simulation, this network requires a typical circuit solution with number of nodes proportional to the number of physical elements (TPSs and vehicles). In this arrangement, the system equations are not unique due to the change of position over time.

Modified nodal analysis (MNA) is used to perform the circuit solution [42]. The vehicle subsystem is considered as a known voltage source. The TPS, alternates between a known voltage source and current source in function of its operating state. The topology and admittance values in the solution matrix are recalculated at each integration step given by (23). Also, for the MNA solution the connection resistance of the vehicle r_{vh} and TPS r_{ss} are included in series. The MNA has thus to couple all other elements (Fig. 6).

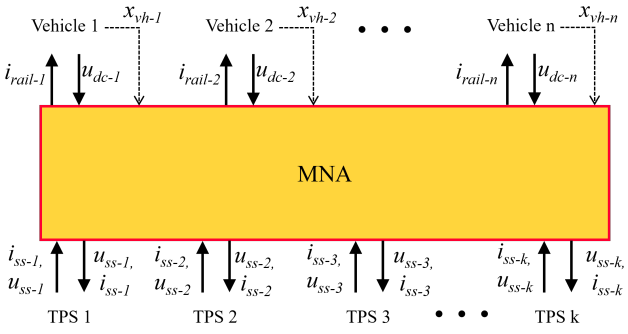

Fig. 6. MNA coupling all other elements.

III. Experimental Validation

The model and control of the vehicle are implemented in Matlab Simulink©. Further, experimental results are taken by running the vehicle on Line 1 in the city of Lille, France. The parameters of the vehicle are given in TABLE I.

TABLE I
SUBWAY PARAMETERS

Parameter		Value
Dynamical Mass		60.9 [t]
Dynamical Mass occupation of 4 p/m^2	M_{vh}	81.7 [t]
Dynamical Mass occupation of 6 p/m^2		88.6 [t]
Filter Capacitance	C_{bus}	7800 [μF]
Rail rated Voltage	v_{rl}	850 [V]
Radius of the Wheel	R_{wh}	0.467 [m]
Differential Gear Ratio	K_d	8.2
Differential Gear Efficiency	η_d	0.955
Auxiliary Power	P_{aux}	3.2 [kW]
Electrical Drive Efficiency	η_{dr}	0.90
Linear Resistance	Λ_{rail}	22 [$\mu\Omega$/m]

For comparison of experimental and simulation results, the measured velocity profile is imposed to the model (Fig. 7). Also, the line topology conditions are respected according to reality, such as slope and tunnel effect.

A. Global Non-receptive Line

A first test is realized during the night between different passenger stations (Fig. 7a). As there is a unique vehicle in this test, there is no energy recovery (non-receptive line) and the traction current is always positive (Fig. 7b). The measured velocity is applied to the simulation model. The average error between the measured and simulated current is 10A, despite some peaks in transients (Fig. 7c).

The DC bus voltage has great variations, specifically during braking (Fig. 7d). This behavior confirms the need to consider this voltage in the model. When the voltage reach its maximal value the TPS is blocked and the mechanical brake is activated. Despite this great variations and modes, the energy consumption error with the simulation is lower than 2.2% (Fig. 7e). The global model is thus validated for a complete line with different velocity patterns, slopes and stop times, but for a non-receptive line (no energy recovery).

B. Interstation Travel with a Receptive Line

Another experimental test is achieved, with a receptive line during the day: as many vehicles circulate, energy recovery is possible. Only an interstation travel is presented for a given velocity (Fig. 8a). The current has now a negative value because of energy transfer to another vehicle which accelerates (Fig. 8c). The energy consumption error is still about 2% (Fig. 8e) but the energy recovery is now highlighted: in that travel, 51% of energy is recovered. The model is thus capable of describing energy transfer between different vehicles.

During a typical acceleration and braking profile, an important electrical power demand is observed. Fig. 8f presents experimental values obtained from the product between voltage (u_{dc}) and current (i_{rail}) at the subway connection point.

The maximal power observed is around 1.4 MW, however, due to energy recovery phase the average value for this trip is only 230 kW. This result agrees with the resulted energy consumption measured.

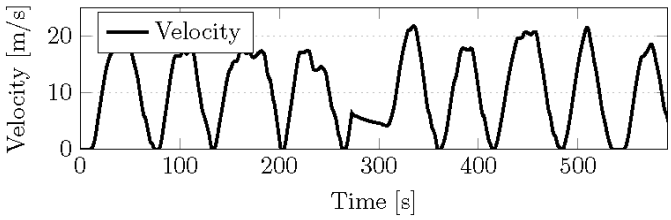

(a) Vehicle velocity.

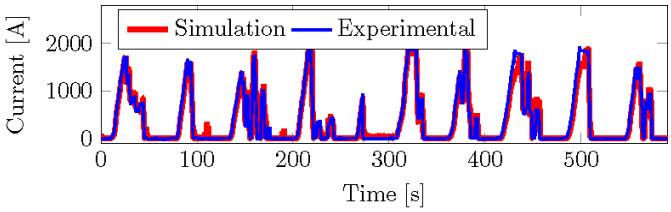

(b) Experimental and measured currents.

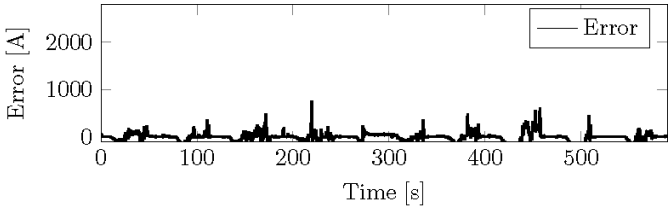

(c) Current error.

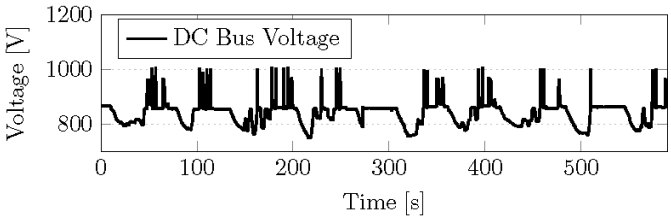

(d) DC bus voltage.

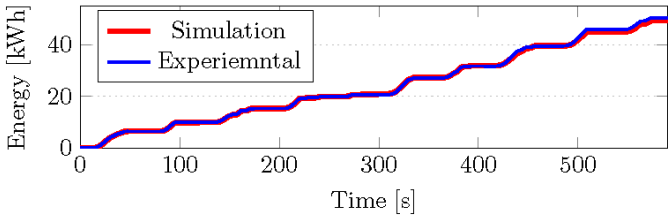

(e) Energy consumption.

Fig. 7. Comparison between experimental measurements and simulations.

IV. STUDY OF DIFFERENT TIME INTERVALS

In the operation of a subway line, vehicles are regularly injected into the system to respect a certain time interval. This time interval is called headway. Currently, on Line 1 of the city of Lille, this interval varies in normal operation between 66 seconds in rush hours and 360 seconds in the early morning or late evening. In some operations, the headway can be reduced to 50s. The impact on the selection of a given time interval between vehicles is analyzed in this section using the model previously developed. For a wider evaluation, intervals between 50 and 360 seconds are selected for this study. As

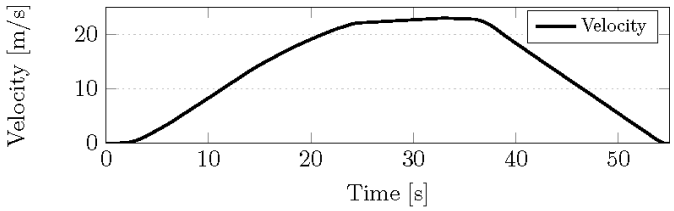

(a) Vehicle velocity.

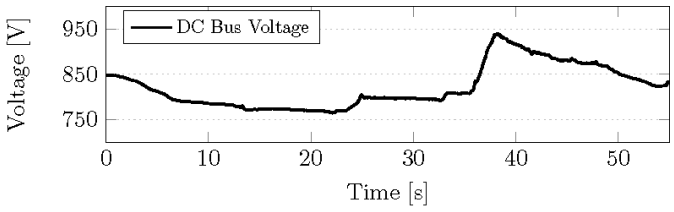

(b) DC bus voltage.

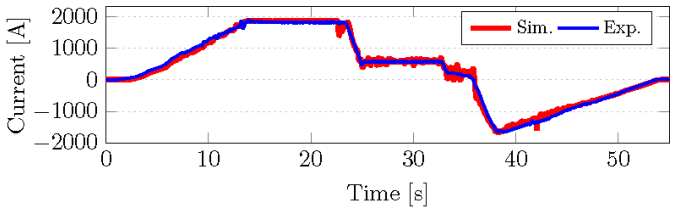

(c) Experimental and measured currents.

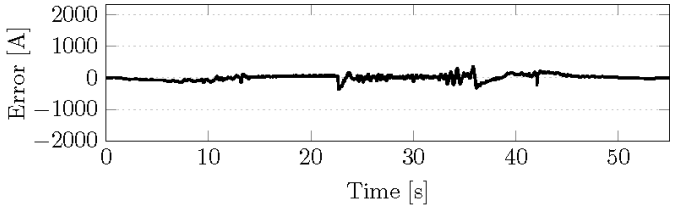

(d) Current error.

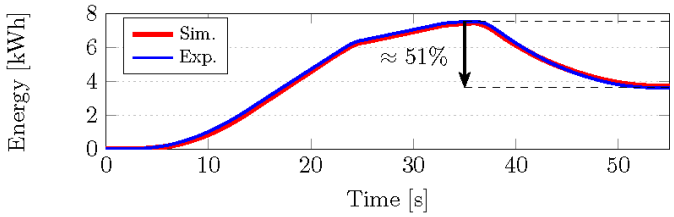

(e) Experimental and measured energy consumptions.

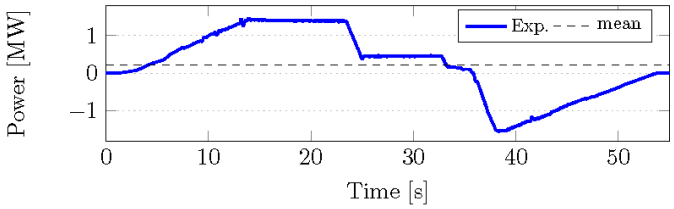

(f) Electrical power demand

Fig. 8. Comparison between experimental measurements and simulations.

the distance between the stations is not regular in a real line, and the time interval is regular, it is difficult to analyze the global energy consumption. In the first step, a fictitious line with regular time intervals and station distances is studied. The real line is analyzed in a second time.

Peak-hours have an important impact on energy consumption [18]. Not only the number of vehicles is greater, but also the mass to be transported due to the increase in the number of users. Simulations are performed for different intervals and two occupancy rate scenarios are considered. In each simulated interval the total vehicle mass is fixed according to the assigned number of occupants.

A. Fictitious Line with Regular Distances

The fictitious line has regular distance between TPS and regular distance between passenger stations. The main idea is to avoid effect of the distances when varying the time interval (headway). In that way, we can better analyze the effect of the time interval on the energy consumption.

A segment composed of 4 TPSs and 4 passenger stations is proposed. The distances between stations and TPSs are chosen with reference to the average values of the distances of the real line (TABLE II). Moreover, the stop time at each passenger station is also considered the same for any station (average value of the stop times of the real line).

TABLE II
FICTITIOUS LINE PARAMETERS

Parameter	Value
Distance between TPS	1083 [m]
Distance between Station	650 [m]
Stop Time	16 [s]
Linear Resistance	22 [$\mu\Omega$/m]
Maximal Velocity	60 [km/h]

Simulations are conducted by analyzing vehicle time intervals ranging from 50 to 360 seconds. To facilitate comparison, energy consumption per passenger-kilometer, denoted as [Wh/pkm], is employed as the standard unit, which is commonly used in transportation systems. In this paper, it is referred as consumption. In order to verify the influence of the mass variation on the consumption, two occupancy rates are considered, 4 and 6 passengers per square meter $\left[\mathrm{p/m^2}\right]$. These occupancy rates are representative values of the subway of the city of Lille.

Fig. 9 presents the consumption considering the studied intervals. First, an oscillatory pattern with local maxima and minima is identified. The minima occur when the number of subway braking is close to the number of subways accelerating: most of the energy recovery can be reused by an accelerating subway. The maxima occur when the number of subway braking is far from the number of subways accelerating: most of the braking energy is dissipated by mechanical brakes. Second, except for this oscillatory pattern, the more the headway is, the more energy consumption is. For high headway, the distance between the vehicle is important and the energy transmission is lower due to the losses in the rail.

In practice, this figure illustrates the optimal time intervals for minimizing energy consumption, as well as the intervals that should be avoided to effectively limit energy consumption. It can be noted a decrease of 30% between the minimal value (headway of 57s) and the local maximal value (headway of 61s). In conclusion for this fictitious line, a headway of 57s can significantly reduce energy consumption.

In general, the observed oscillatory pattern can be attributed to the synchronization of the braking and acceleration phases among the vehicles circulating in the line. This synchronization is particularly important at specific time intervals.

In Fig. 10, different occupancy rates are considered. If the global energy consumption is greater for 6 p/m^2 than for 4 p/m^2 (more important mass), the consumption per passenger-kilometer is lower for 6 p/m^2. If more energy is used, more passengers are transported. However, the oscillatory pattern is conserved, and the maxima and minima are located for the same time intervals. That means that the selection of the best headway in terms of energy consumption is independent of the occupancy rate.

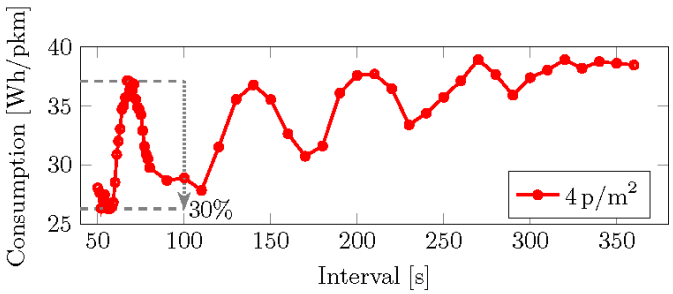

Fig. 9. Energy consumption vs. headway for a fictitious line.

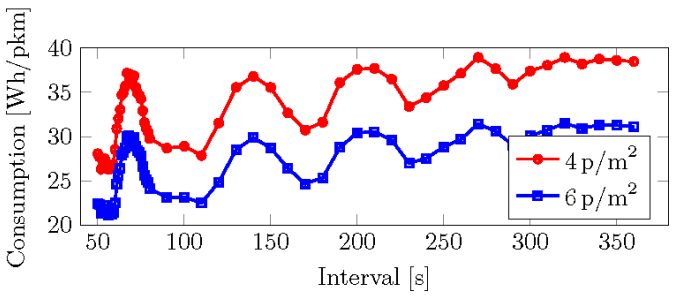

Fig. 10. Different occupation rates vs. consumption for a fictitious line.

The fictitious line demonstrates an important impact of the time interval between vehicles on energy consumption. A specific value of the headway can lead to a significant reduction in the total energy consumption. As this effect is independent of the occupancy rate, an optimal headway could be selected for normal operation.

B. Real Line Study

The same analysis is applied to a real line. A section of Line 1 of the city of Lille, France, is used. In this case, the slope and tunnel effects are also considered. The positions of substations and passenger stations are not regularly distributed (TABLE III). The stopping time at the passenger stations is also different depending on the average number of passengers for each station.

TABLE III
REAL LINE PARAMETERS

TPS	Position	Station	Position	Time of stop
TPS 1	0 [m]	4 Cantons	417 [m]	16 [s]
TPS 2	260 [m]	Cité Scientifique	1193 [m]	14 [s]
TPS 3	1780 [m]	Triolo	2020 [m]	12 [s]
TPS 4	3394 [m]	Hôtel de Ville	2703 [m]	16 [s]

Fig. 11 presents the energy consumption as a function of the time interval. An oscillatory pattern is also observed, but with a more irregular shape. This irregularity can be attributed to the inconsistent distances between TPS or passenger stations, resulting in less uniform braking phases. Regardless, the developed model is capable of simulating various scenarios. Local maxima and minima indicate intervals that could be prioritized or avoided concerning energy consumption. The decrease between the maximal energy consumption (headway 67s) and the minimal one (headway 57s) is only 22% compared to 30% of the fictitious regular line. But, the difference is still important and the selection of a relevant headway can significantly reduce the total energy consumption. As this potential energy gain is related to a difference of 10s of headway, it seems possible to select the best headway for some slot times in the day. The occupancy rates have an impact on the total energy consumption but no impact on the minima and maxima, as observed in the case of the fictitious line.

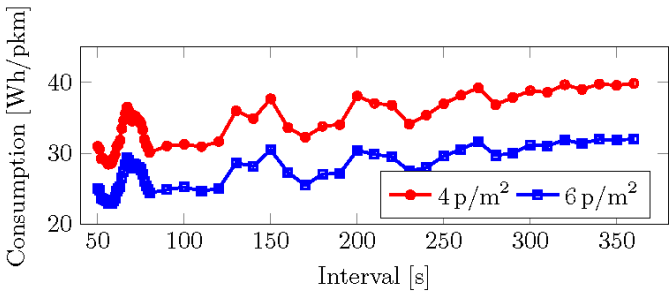

Fig. 11. Energy consumption vs. headway for a real line.

In the real line, it is also possible to observe that low consumption values can only be achieved in a line with high vehicle traffic.

The consumption trends are similar for both the fictitious and the real line. In the former, a uniform pattern of local maxima and minima is observed, while in the latter, an irregular pattern is seen. Despite the irregularity, local maxima and minima are still present. It is indeed possible to significantly reduce energy consumption on a real line by optimizing time intervals. However, obtaining a theoretical solution is challenging due to factors such as TPS distances, passenger station distances, slopes, and more. Consequently,

an accurate simulation model is valuable for addressing these complexities.

The local maxima and minima values are related to operational variables such as maximal velocity, stopping time, and distance between stations. For other lines the values can be found in other headways. This fact reinforces the need for accurate simulation tools in order to identify good operating points.

V. Conclusion

The analysis of the impact of timetable on the global energy consumption of a subway line is performed. To ensure an accurate estimation of global energy consumption, the models of each subsystem are developed in a forward approach using the EMR formalism. Moreover, the dynamic of the input filter capacitor is considered as its voltage impacts the braking strategy and thus the potential energy recovery. The new subway model has been validated by experimental tests on a real subway line. The simulation model has an error lower than 2.2% on energy consumption.

The model is then used to estimate the energy consumption for different time intervals between the vehicles. For a first analysis, a fictitious line is considered with constant distances between the TPS and also the passenger stations. The change in the time interval leads to a strong reduction in energy consumption due to the indirect synchronization of the subways. When the number of subways decelerating is close to the one of the subways accelerating, the energy consumption is significantly reduced because of the transfer of the braking energy. The study is extended to a real line with non-regular distances. Moreover, the slopes and the real stopping times are also considered. In this realistic study case, the global energy consumption can be decreased by 22% between the best time interval and the worse time interval. An oscillatory pattern is obtained from the energy consumption vs. the time interval. It shows the time intervals that are of interest for the reduction of energy consumption, but also the time intervals to be avoided. Moreover, the dissipated energy is also plotted vs. the time interval. Another oscillatory pattern is obtained, showing the potential of recovery energy for new saving technologies.

The presented modeling approach introduces a comprehensive methodology for evaluating the impact of the timetable on energy consumption in subway systems. By taking into account different traffic conditions with intervals of 50 and 60 seconds, the current study provides a solid foundation for future optimization efforts. It is important to note that with the developed flexible simulation tool more complex timetables can be considered. It will be analyzed in further steps.

Future work will focus on refining the algorithms and strategies used for timetable optimization, incorporating the influence of the occupancy rate, and exploring other relevant variables that may impact energy consumption. The ultimate goal is to develop a comprehensive framework that will enable transportation planners and operators to simulate optimization techniques that minimize energy consumption while ensuring an efficient and reliable subway system.

Acknowledgments

The research leading to these results has received funding from the European Metropole of Lille and the "Hauts-de-France" region within the CUMIN-REMUS project.

References

[1] UITP Advancing Public Transport, *World Metro Figures 2021*, May 2022 2022.

[2] IEA (International Energy Agency), *The Future of Rail - Opportunities for energy and the environment*, Jan. 2019.

[3] M. Shang, Y. Zhou, Y. Mei, J. Zhao, and H. Fujita, "Energy-saving train operation synergy based on multi-agent deep reinforcement learning on spark cloud," *IEEE Transactions on Vehicular Technology*, vol. 72, no. 1, pp. 214–226, 2023.

[4] J. Liu, H. Guo, and Y. Yu, "Research on the cooperative train control strategy to reduce energy consumption," *IEEE Transactions on Intelligent Transportation Systems*, vol. 18, no. 5, pp. 1134–1142, 2017.

[5] P. Arboleya, C. Mayet, B. Mohamed, J. A. Aguado, and S. de la Torre, "A review of railway feeding infrastructures: Mathematical models for planning and operation," *eTransportation*, vol. 5, p. 100063, 2020.

[6] M. Khodaparastan, O. Dutta, M. Saleh, and A. A. Mohamed, "Modeling and simulation of dc electric rail transit systems with wayside energy storage," *IEEE Transactions on Vehicular Technology*, vol. 68, no. 3, pp. 2218–2228, 2019.

[7] F. Hao, G. Zhang, J. Chen, and Z. Liu, "Distributed reactive power compensation method in dc traction power systems with reversible substations," *IEEE Transactions on Vehicular Technology*, vol. 70, no. 10, pp. 9935–9944, 2021.

[8] Q. Qin, T. Guo, F. Lin, and Z. Yang, "Energy transfer strategy for urban rail transit battery energy storage system to reduce peak power of traction substation," *IEEE Transactions on Vehicular Technology*, vol. 68, no. 12, pp. 11 714–11 724, 2019.

[9] A. Allègre, A. Bouscayrol, P. Delarue, P. Barrade, E. Chattot, and S. El-Fassi, "Energy storage system with supercapacitor for an innovative subway," *IEEE Transactions on Industrial Electronics*, vol. 57, no. 12, pp. 4001–4012, 2010.

[10] Z. Zhong, Z. Yang, X. Fang, F. Lin, and Z. Tian, "Hierarchical optimization of an on-board supercapacitor energy storage system considering train electric braking characteristics and system loss," *IEEE Transactions on Vehicular Technology*, vol. 69, no. 3, pp. 2576–2587, 2020.

[11] F. Meishner and D. U. Sauer, "Wayside energy recovery systems in dc urban railway grids," *eTransportation*, vol. 1, p. 100001, 2019.

[12] S. Su, T. Tang, X. Li, and Z. Gao, "Optimization of multitrain operations in a subway system," *IEEE Transactions on Intelligent Transportation Systems*, vol. 15, no. 2, pp. 673–684, 2014.

[13] H. Liu, M. Zhou, X. Guo, Z. Zhang, B. Ning, and T. Tang, "Timetable optimization for regenerative energy utilization in subway systems," *IEEE Transactions on Intelligent Transportation Systems*, vol. 20, no. 9, pp. 3247–3257, 2019.

[14] M. Botte, L. D'Acierno, and M. Pagano, "Impact of railway energy efficiency on the primary distribution power grid," *IEEE Transactions on Vehicular Technology*, vol. 69, no. 12, pp. 14 131–14 140, 2020.

[15] S. Su, X. Wang, Y. Cao, and J. Yin, "An energy-efficient train operation approach by integrating the metro timetabling and eco-driving," *IEEE Transactions on Intelligent Transportation Systems*, vol. 21, no. 10, pp. 4252–4268, 2020.

[16] C. Liebchen, "The first optimized railway timetable in practice," *Transportation Science*, vol. 42, no. 4, pp. 420–435, 2008.

[17] E. Barrena, D. Canca, L. C. Coelho, and G. Laporte, "Single-line rail rapid transit timetabling under dynamic passenger demand," *Transportation Research Part B: Methodological*, vol. 70, pp. 134–150, 2014.

[18] J. Yin, A. D'Ariano, Y. Wang, L. Yang, and T. Tang, "Timetable coordination in a rail transit network with time-dependent passenger demand," *European Journal of Operational Research*, vol. 295, no. 1, pp. 183–202, 2021.

[19] J. Yuan, Y. Gao, S. Li, P. Liu, and L. Yang, "Integrated optimization of train timetable, rolling stock assignment and short-turning strategy for a metro line," *European Journal of Operational Research*, vol. 301, no. 3, pp. 855–874, 2022.

[20] Y. Huang, L. Yang, T. Tang, F. Cao, and Z. Gao, "Saving energy and improving service quality: Bicriteria train scheduling in urban rail transit systems," *IEEE Transactions on Intelligent Transportation Systems*, vol. 17, no. 12, pp. 3364–3379, 2016.

[21] P. Liu, L. Yang, Z. Gao, Y. Huang, S. Li, and Y. Gao, "Energy-efficient train timetable optimization in the subway system with energy storage devices," *IEEE Transactions on Intelligent Transportation Systems*, vol. 19, no. 12, pp. 3947–3963, 2018.

[22] X. Yang, X. Li, Z. Gao, H. Wang, and T. Tang, "A cooperative scheduling model for timetable optimization in subway systems," *IEEE Transactions on Intelligent Transportation Systems*, vol. 14, no. 1, pp. 438–447, 2013.

[23] I. E. Demirci and H. B. Celikoglu, "Timetable optimization for utilization of regenerative braking energy: A single line case over istanbul metro network," in *2018 21st International Conference on Intelligent Transportation Systems (ITSC)*, 2018, pp. 2309–2314.

[24] P. Mo, L. Yang, A. D'Ariano, J. Yin, Y. Yao, and Z. Gao, "Energy-efficient train scheduling and rolling stock circulation planning in a metro line: A linear programming approach," *IEEE Transactions on Intelligent Transportation Systems*, vol. 21, no. 9, pp. 3621–3633, 2020.

[25] C. Zhu, G. Du, X. Jiang, W. Huang, D. Zhang, M. Fan, and Z. Zhu, "Dual-objective optimization of maximum rail potential and total energy consumption in multitrain subway systems," *IEEE Transactions on Transportation Electrification*, vol. 7, no. 4, pp. 3149–3162, 2021.

[26] G. Caimi, L. Kroon, and C. Liebchen, "Models for railway timetable optimization: Applicability and applications in practice," *Journal of Rail Transport Planning & Management*, vol. 6, no. 4, pp. 285–312, 2017.

[27] P. Liu, M. Schmidt, Q. Kong, J. C. Wagenaar, L. Yang, Z. Gao, and H. Zhou, "A robust and energy-efficient train timetable for the subway system," *Transportation Research Part C: Emerging Technologies*, vol. 121, p. 102822, 2020.

[28] J. Xun, T. Liu, B. Ning, and Y. Liu, "Using approximate dynamic programming to maximize regenerative energy utilization for metro," *IEEE Transactions on Intelligent Transportation Systems*, vol. 21, no. 9, pp. 3650–3662, 2020.

[29] Y. Bai, Y. Cao, Z. Yu, T. K. Ho, C. Roberts, and B. Mao, "Cooperative control of metro trains to minimize net energy consumption," *IEEE Transactions on Intelligent Transportation Systems*, vol. 21, no. 5, pp. 2063–2077, 2020.

[30] P. Luo, Q. Li, Y. Zhou, Q. Ma, Y. Zhang, Y. Peng, and J. Sun, "Multi-application strategy based on railway static power conditioner with energy storage system," *IEEE Transactions on Intelligent Transportation Systems*, vol. 22, no. 4, pp. 2140–2152, 2021.

[31] C. Mayet, A. Bouscayrol, P. Delarue, E. Chattot, and J. N. Verhille, "Electrokinematical simulation for flexible energetic studies of railway systems," *IEEE Transactions on Industrial Electronics*, vol. 65, no. 4, pp. 3592–3600, 2018.

[32] C. Mayet, P. Delarue, A. Bouscayrol, E. Chattot, and J. Verhille, "Comparison of different emr-based models of traction power substations for energetic studies of subway lines," *IEEE Transactions on Vehicular Technology*, vol. 65, no. 3, pp. 1021–1029, 2016.

[33] W. Wang, M. Cheng, Y. Wang, B. Zhang, Y. Zhu, S. Ding, and W. Chen, "A novel energy management strategy of onboard supercapacitor for subway applications with permanent-magnet traction system," *IEEE Transactions on Vehicular Technology*, vol. 63, no. 6, pp. 2578–2588, 2014.

[34] R. O. Berriel, P. Delarue, A. Bouscayrol, and C. Brocart, "Model simplifications of a subway vehicle for computation of energy consumption," in *2021 IEEE Vehicle Power and Propulsion Conference (VPPC)*, 2021, pp. 1–5.

[35] C. Mayet, L. Horrein, A. Bouscayrol, P. Delarue, J.-N. Verhille, E. Chattot, and B. Lemaire-Semail, "Comparison of different models and simulation approaches for the energetic study of a subway," *IEEE Transactions on Vehicular Technology*, vol. 63, no. 2, pp. 556–565, 2014.

[36] R. O. Berriel, A. Bouscayrol, P. Delarue, and C. Brocart, "Mechanical braking strategy impact on energy consumption of a subway," in *2020 IEEE Vehicle Power and Propulsion Conference (VPPC)*, 2020, pp. 1–5.

[37] A. Bouscayrol, J.-P. Hautier, and B. Lemaire-Semail, *Graphic Formalisms for the Control of Multi-Physical Energetic Systems: COG and EMR*. John Wiley & Sons, Ltd, 2013, ch. 3, pp. 89–124.

[38] P. Arboleya, C. Mayet, A. Bouscayrol, B. Mohamed, P. Delarue, and I. El-Sayed, "Electrical railway dynamical versus static models for infrastructure planning and operation," *IEEE Transactions on Intelligent Transportation Systems*, vol. 23, no. 6, pp. 5514–5525, 2022.

[39] S. Chiniforoosh, H. Atighechi, and J. Jatskevich, "A generalized methodology for dynamic average modeling of high-pulse-count rectifiers in transient simulation programs," *IEEE Transactions on Energy Conversion*, vol. 31, no. 1, pp. 228–239, 2016.

[40] C. Mayet, P. Arboleya, A. Bouscayrol, B. Mohamed, P. Delarue, and I. El-Sayed, "Non-linear switched model for accurate voltage estimation and power flow analysis of dc railway systems," *IET Electrical Systems in Transportation*, vol. 10, no. 4, pp. 425–435, 2020.

[41] B. Mohamed, P. Arboleya, and C. González-Morán, "Modified current injection method for power flow analysis in heavy-meshed dc railway networks with nonreversible substations," *IEEE Transactions on Vehicular Technology*, vol. 66, no. 9, pp. 7688–7696, 2017.

[42] C.-W. Ho, A. Ruehli, and P. Brennan, "The modified nodal approach to network analysis," *IEEE Transactions on Circuits and Systems*, vol. 22, no. 6, pp. 504–509, 1975.